Applied Catalysis B: Environmental 140–141 (2013) 225–232

Contents lists available at SciVerse ScienceDirect

Applied Catalysis B: Environmental

journal homepage: www.elsevier.com/locate/apcatb

Comparative studies of photocatalytic and photoelectrocatalytic inactivation of *E. coli* in presence of halides

Guiying Li[a,b], Xiaolu Liu[a,b], Haimin Zhang[b], Po-Keung Wong[c], Taicheng An[a,*], Huijun Zhao[b,**]

[a] State Key Laboratory of Organic Geochemistry, Guangzhou Institute of Geochemistry, Chinese Academy of Sciences, Guangzhou 510640, PR China
[b] Centre for Clean Environment and Energy, Gold Coast Campus, Griffith University, Queensland 4222, Australia
[c] School of Life Sciences, The Chinese University of Hong Kong, Shatin, N.T., Hong Kong Special Administrative Region, China

ARTICLE INFO

Article history:
Received 7 January 2013
Received in revised form 30 March 2013
Accepted 1 April 2013
Available online 8 April 2013

ABSTRACT

The bactericidal performances of photocatalytic and photoelectrocatalytic systems in absence and presence of low concentrations of X^- (X = Br, Cl) were quantitatively studied and meaningfully compared under identical experimental conditions. The photoelectrocatalytic system in presence of low concentration of Br^- was found to be the most effective bactericidal system amongst all systems investigated, capable of inactivating 100% of 9.0×10^6 CFU/mL *Escherichia coli* within 1.57 s. The photocatalytically generated active oxygen species are important attributes to the bactericidal performance of all cases investigated except the case of photoelectrocatalytic inactivation in presence of Br^- for which the bactericidal performance is dominated by the photoelectrocatalytically generated $Br^{\bullet-}/Br_2^{\bullet-}$. The results revealed that in a photocatalysis or photoelectrocatalysis bactericidal process, X^- acts as an electron mediator that does not change its chemical form before and after bactericidal process, and a high bactericidal performance photoelectrocatalytic system can be established with Br^- concentration as low as 50 μM. The findings of this work confirm that new forms of effective bactericides such as $X^{\bullet-}/X_2^{\bullet-}$ can be generated in situ via a photocatalysis or photoelectrocatalysis process for high performance bactericidal system.Keywords: Biohazards; Disinfection; $Br^{\bullet-}/Br_2^{\bullet-}$; Photocatalysis; Photoelectrocatalysis

1. Introduction

Uncertain global climatic conditions, ever increased population growth and rapid industrialization have placed enormous pressure on traditional freshwater sources. To encounter the situation, the recently developed water security strategies have considered the purified recycled wastewater (PRW) as a reliable freshwater source to increase the water supply capacity, especially in large cities [1–3]. Currently, membrane technologies are almost exclusively employed for all large scale PRW productions [4–6]. These membrane-based PRW production systems normally involve the use of microfiltration, ultrafiltration and reverse osmosis membranes in sequence to remove contaminants [5,6]. These membranes are made of polymeric materials. Although the chlorination has been the most widely used disinfection technique, it is unsuitable for membrane-based PRW production because a long-term contact to a source solution containing chlorine residuals can severely damage these polymeric membranes. As a result, the membrane-based PRW production system requires the use of a disinfection technique that does not produce long-lived oxidative residuals. In this regard, the photocatalysis-based techniques could meet the needs.

The illuminated TiO_2, especially the nanostructured TiO_2 has demonstrated to be effective to remove organic contaminants. In 1985, Matsunaga and co-workers have reported for the first time that such a photocatalysis system can also be used to sterilize bacteria and yeast [7]. A large body of work has since been carried out. Up till now, the photocatalytic inactivation of a wide range of microorganisms has been reported [8–16]. In their initial study, Matsunaga and co-workers investigated the photocatalytic disinfection of *Escherichia coli*, *Lactobacillus acidophilus* and *Sacharomyces cerevisae* using TiO_2/Pt as the photocatalyst [7]. They observed that the coenzyme A was oxidized after 120 min under near-UV irradiation and therefore proposed that the inhibited cellular respiratory activity resulted from the photocatalytic damages to the coenzyme A was the cause for the cell death. A subsequent study by Saito and co-workers proposed that the cell death may be caused by the damages to the cell wall and inner membrane [17]. They suggested that the punctures resulted from the attack by the photocatalytically generated $^{\bullet}OH$ radicals lead to a rapid K^+ leakage and release of protein and RNA, responsible for the cell death.

* Corresponding author. Tel.: +86 20 85291501; fax: +86 20 85290706.
** Corresponding author. Tel: +61 7 555 2 8261; fax: +61 7 5552 8067.
E-mail addresses: antc99@gig.ac.cn (T. An), h.zhao@griffith.edu.au (H. Zhao).

0926-3373/$ – see front matter © 2013 Elsevier B.V. All rights reserved.
http://dx.doi.org/10.1016/j.apcatb.2013.04.004

These processes could also involve in the attack to the intracellular macromolecules such as nucleic acids [18]. These are similar to the killing mechanism proposed by Sunada and co-workers [19]. They suggested that the cell killing mechanism involves in an initial partial decomposition of the outer cell membrane followed by disordering of the cytoplasmic membrane by the photocatalytically generated active oxygen species (AOSs). The damages to the cell membrane were evidenced by an attenuated total reflection Fourier transform infrared spectroscopic study of *E. coli* cell wall structural change during TiO_2 photocatalysis process [20] and by monitoring the malondialdehyde formation to determine the cell wall lipid peroxidation [21,22]. Despite the significant progress, some details of killing mechanisms are still under investigation. Nevertheless, there has been a commonly accepted view that the bactericidal effect of TiO_2 photocatalysis is achieved via the photocatalytically generated AOSs [9,11,13]. These AOSs possess a shorter life in aqueous environments and less effective to cause damage to the polymeric membrane materials [10,13,23].

While the photocatalysis-based techniques could suit the needs for membrane-based PRW production systems, their disinfection efficiency needs to be improved before practical use [24–27]. High rate of electron-hole recombination in a photocatalytic (PC) system has been one of the significant attributes for the low photocatalytic efficiency, hence the low photocatalytic disinfection efficiency. This can be encountered by employing a photoelectrocatalytic (PEC) system [23,28–32]. A PEC system allows the application of a potential bias to rapidly remove the photocatalytically generated electrons from the TiO_2 conduction-band to the counter electrode (where the reduction-half reactions occur), suppressing the recombination [30]. Although the PEC approach has been widely used for detoxification and degradation of organic pollutants [30,33], its application for disinfection of microbes is the least exploited with only a few scattered reports [23,28]. The first electric field enhanced photochemical reactor for enhancement of disinfection efficiency was reported by Butterfield and co-workers [34]. They demonstrated that 3 log units (100%) of *E. coli* and 2 log units of *CI. perfringens* spores can be inactivated within 25 min by UV illuminated TiO_2. Significantly enhanced inactivation efficiency toward MS-2 bacteriophage by employing a PEC reactor was recently reported [28]. It should be noted that for a PC system, the photocatalytically generated AOSs are the essential bactericides responsible for killing, while for a PEC system, the photocatalytically generated holes (with greater oxidation power than that of AOSs) can directly act as a bactericide (in addition to AOSs) because the suppressed recombination prolongs the life of photoholes [23].

As aforementioned, all reported PC-based bactericidal systems rely on the photocatalytically generated AOSs to achieve inactivation. However, the short life of AOSs in aqueous environment is another important attribute that limits the inactivation efficiency of PC-based bactericidal systems. To this end, we recently reported a PEC-based bactericidal system capable of in situ generating non-AOS forms of bactericides [23]. In presence of low concentration of Br^-, relatively long-lived di-bromide radical anions ($Br_2^{\bullet -}$) can be produced and served as effective bactericides. This PEC bactericidal system, namely, PEC–Br system, utilizes the combined effect of $Br_2^{\bullet -}$, h^+ and AOSs (see Eq. (1)) to achieve instantaneous inactivation and rapid decomposition [23].

$$TiO_2\{h_{VB}^+\}/\{Br^\bullet/Br_2^{\bullet -}\}/\{AOS\} \xrightarrow{\text{Bacteria}} \text{Oxidized bacteria} \quad (1)$$

In such a PEC–Br bactericidal process, Br^- acts as an "electron mediator" that does not change its chemical form before and after bactericidal process [23]. Br^- is firstly photoelectrocatalytically oxidized to $Br_2^{\bullet -}$ that reacts with Br^- to form $Br_2^{\bullet -}$ (see Eq. (2)), and then regenerated when $Br^\bullet$ and $Br_2^{\bullet -}$ are reduced by bacteria or other reduction reagents (see Eq. (3)). This is important for a membrane-based PRW production process as no long-lived oxidative residuals will be remained in the PEC–Br treated solution.

$$Br^\bullet + Br^- \rightarrow Br_2^{\bullet -} \quad (2)$$

$$Br^\bullet/Br_2^{\bullet -} \xrightarrow{\text{Bacteria}} Br^- + \text{Oxidized bacteria} \quad (3)$$

The proof of concept and investigating the inactivation/decomposition mechanisms in presence of Br^- were the main focuses of our previous work [23]. This work extends the investigation to include Cl^-. F^- and I^- are unsuitable for photocatalysis-based bactericidal applications because F^- ($E^0[F^\bullet/F^-] = +3.6$ V) [35] cannot be photocatalytically oxidized to $F^\bullet$ by the illuminated TiO_2 while $I^\bullet$ ($E^0[I^\bullet/I^-] = +1.33$ V) [36] possesses insufficient oxidation power for inactivation. Detailed investigations were carried out to understand the effect of halides presence on the bactericidal performance of photocatalytic (PC–X) and photoelectrocatalytic (PEC–X) inactivation efficiency. This would be the first time the bactericidal performance of PC and PEC systems is meaningfully compared under comparable experimental conditions.

2. Experimental

2.1. Materials

Indium tin oxide conducting glass slides (ITO, 8 Ω/square) were purchased from Delta Technologies Ltd. (USA). Titanium butoxide (97%, Aldrich), Nutrient Broth (Oxoid) and Nutrient agar (Oxoid), were used as received. As representatives of Gram-negative bacteria, strain of *E. coli* K12 was purchased from Southern Biological. Other chemicals used were of analytical grade and purchased from Sigma unless otherwise stated. All solutions were prepared using high purity deionized water (Millipore Corp., 18 MΩ cm).

2.2. UV-LED array photoelectrochemical cell

All PC and PEC disinfection experiments were performed in a continuous flow-through photoelectrochemical thin layer cell with a quartz window for illumination. The cell consists of a TiO_2 photoanode as the working electrode, a Ag/AgCl reference electrode and a Pt disc auxiliary electrode. The TiO_2 photoanode was prepared by hydrolysis of titanium butoxide according to the method described in our previous work [37]. The resultant photoanode was a clear three-layer structure that compresses a thick glass substrate layer, a 200 nm compact ITO conductive layer coated on the glass substrate and a 2 μm porous TiO_2 nanoparticle layer deposited on the top of the ITO conductive layer. The TiO_2 nanoparticles (sized from 30 to 50 nm) consist of 96.6% anatase and 3.4% rutile. The thickness of the reaction chamber, the illumination area and the volume of the compartment were 0.25 mm, 462 mm^2 and 115.5 mm^3, respectively. The illumination source was a UV-LED array which consisted of single cross 4 pieces of UV-LED (NCCU033 (T), Nichia Corporation). The specified peak wavelength of the LED was 365 nm with a spectrum half width of 8 nm. The UV intensity on the electrode surface was 8.0 mW cm^{-2} measured with an UV-irradiance meter (UV-A, Beijing Normal University), and can be adjusted by a power supply.

2.3. Bacterial culture conditions and cell preparation

The bacterial strain used was inoculated into nutrient broth and grown overnight at 37 °C by constant agitation under aerobic conditions. After incubation, for the suspension system, bacterial cells were harvested by centrifugation at 3000 rpm for 15 min and the bacterial pellet was resuspended in sterile deionized

water. This washing step was repeated three times to eliminate residual substances. Finally, the washed bacterial cells were resuspended in sterile deionized water, and were diluted with sterilized 0.1 M $NaNO_3$ solution to obtain suitable *E. coli* concentrations. For the mechanistic studies, the overnight incubated *E. coli* suspension was seeded, and fresh nutrient broth was also added in a petri dish to allow the cell can multiply and attach to the substrate. The substrates are sterilized TiO_2 photoanodes which were immersed into the petri dish. Subsequently, the enrichment of adhesive microorganisms was incubated at 37 °C for 72 hrs. And the reversible attached cells were washed using sterile deionized water.

2.4. Procedures for disinfection of bacteria

Both PC and PEC disinfection experiments were carried out under identical UV intensity using the same UV-LED array photoelectrochemical cell. For PEC disinfection, a 0.1 M $NaNO_3$ solution was used as the supporting electrolyte. A voltammograph (CV-27, BAS) was used for electrochemical control. Potential and current signals were monitored using a Macintosh computer (7220/200) coupled with a Maclab 400 interface (AD Instruments). A sample containing 9.0×10^6 CFU/ml *E. coli* and 0.1 M $NaNO_3$ was continuously injected into the cell via a precision pump during the disinfection process. The reaction time of a sample was controlled by adjusting the flow rate. A sufficient volume of the reacted sample was collected for further analyses after the system reaching its steady-state for which the obtained sample had been subjected to the same reaction time. A 0.1 M $NaNO_3$ solution was used to clean the cell in between the two sample injections. For the PEC–Br or PEC–Cl disinfection experiments, the test solution with an additional 1.0 mM NaBr or NaCl was employed. PC disinfection experiment was conducted under identical experimental conditions as PEC experiment, except the electrochemical system was disconnected.

2.5. Analysis

To estimate *E. coli* cell viability in the reaction mixture, two sets of experiments were performed. First, *E. coli* cell viability was estimated by means of colony-counting procedure. That is, a sample (200 μl) was withdrawn from the reaction mixture at a given reaction time, followed by spreading on nutrient agar plates after serial dilutions (10^{-1}–10^{-5}) using the saline solution. After incubating the agar plates for 24 hrs at 37 °C in the dark, the developed colonies were enumerated and the number of viable cells was recorded in terms of CFU/mL of the reaction mixture. It should be noted that the data shown in this work were the average values of data obtained from experiments replicated in triplicate. Second, the viabilities of *E. coli* were also evaluated using a commercially available staining kit (Live/Dead Baclight bacterial viability kit, Molecular Probes, Inc.). Staining procedure was carried out as proposed by the manufacturer. Small volume of the stained cell was mounted on a glass slide. The fluorescence microscopy observations and picture capture were performed immediately by using a Nikon digital camera (DS-5Mc, Japan) mounted on an Olympus fluorescence microscope (BX51TR, Japan) and the cells in each image was counted to determine the number of cells on the substrates.

2.6. Scanning electron microscopy

Before and after *E. coli* inactivation, the cell attached to the TiO_2 film slides fixed by 3% glutaraldehyde for approximately 60 min at room temperature, and then washed with 0.1 M cacodylate buffer (pH 7.4) for 10 min and post fixed for 20 min in 1% osmium tetraoxide. Subsequently, the specimens were dehydrated by a graded series of ethanol (70, 90 and 100%) and 100% amyl acetate 2 times each for 10 min, respectively. The cells on the substrates were finally critical point dried by using critical point dryer (Denton Vacuum, Inc. USA), gold sputter coated on the substrates and were visualized using a field emission scanning electron microscope (FESEM, JEOL JSM-6300F).

3. Results and discussion

It is known that halogen radicals are effective bactericides and can be readily produced by photocatalytic oxidation of halide ions at the illuminated TiO_2 surface [38]. The photocatalytically producing high concentration of halogen radicals is possible because some halogen radicals can form stable di-halide radical anions ($X_2^{\bullet -}$) in the presence of X^- [39,40]. Since the effectiveness of a bactericide is highly dependent on its killing mechanisms [41,42], the bactericidal efficiency could be benefited from the different killing mechanisms offered by halide radicals. To simulate these conditions as well as to improve inactivation efficiencies, halide ions were added separately to the bacterial suspension in the PC and PEC disinfection systems. In this work, the bactericidal performance under photocatalytic and photoelectrocatalytic conditions in presence of low concentration of Cl^- and Br^- were investigated. Other halides such as F^- and I^- were excluded because the illuminated TiO_2 is incapable to oxidize F^- ($E^0[F^\bullet/F^-] = +3.6$ V) [35] and the insufficient oxidation power of $I^\bullet$ ($E^0[I^\bullet/I^-] = +1.33$ V) [36] for high bactericidal effect.

3.1. PC Inactivation with and without halide ions

Fig. 1 shows the PC inactivation efficiency of *E. coli* cells as a function of reaction time with or without of chloride/bromide. The bactericidal performance with the TiO_2 and the halides without illumination was carried out as a control. Results showed that the bacterial population remained unchanged within 20 min under the mentioned conditions, suggesting that both treatments had no toxic effect to *E. coli*. For all other photocatalytic treatment, the bacterial population almost remained at a stable value at first 2 min. It is because that various AOSs already begin to attack bacteria but were insufficient to cause a large number of bacterial deaths. With the prolonged reaction time, the cell density decreased gradually. For instance, in the absence of halide ions, approximately 4 log reduction of *E. coli* was achieved after 20 min irradiation. The observed change in cell density with reaction time in presence of 1.0 mM Cl^- (PC–Cl) were found to be similar to that of PC inactivation in absence of halide ions. In the presence of 1.0 mM Br^- (PC–Br), a linearly decreased cell population with reaction time

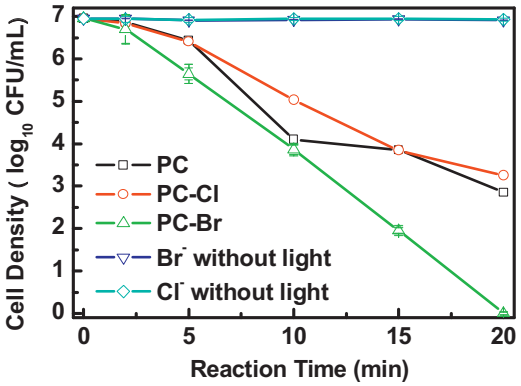

Fig. 1. Survived *E. coli* after different photocatalytic treatment plot against resident time.

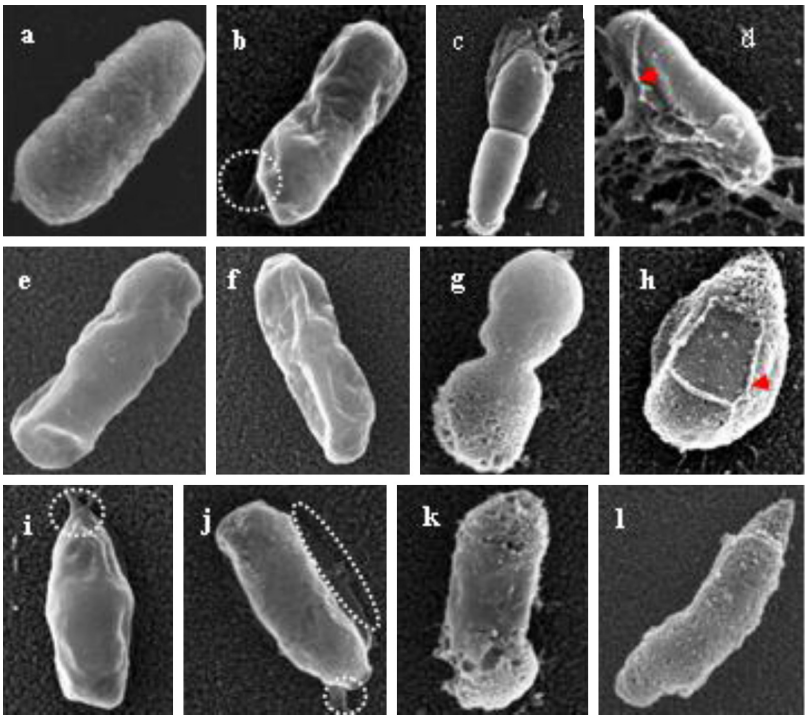

Fig. 2. FESEM images of *E. coli* cell immobilized on the TiO_2 photoanode. (a) Without treatment; (b) after PC 300 s; (c) PC 600 s; (d) PC 900 s; (e) PC–Cl 150 s; (f) PC–Cl 300 s; (g) PC–Cl 600 s; (h) PC–Cl 900 s. (i) PC–Br 150 s; (j) PC–Br 300 s; (k) PC–Br 600 s; and (l) PC–Br 900 s.

was observed after 2 min, and complete inactivation of all bacterial cells will be achieved within 20 min. Compared to PC and PC–Cl treatment, the percentage inactivation obtained from the PC–Br treatment was found to be much higher, reaching 95.1% at 5 min. Although the increase in the percentage inactivation with further reaction time increase was slowed down, a 100% inactivation can still be achieved within 20 min of treatment. This result indicates that under PC treatment conditions, the inactivation efficiency can be significantly increased when a low concentration of Br^- is added. Compared to the PC–Cl treatment, the higher inactivation efficiency of the PC–Br treatment could be attributed to the higher concentration of $Br_2^{\bullet-}$ in the PC–Br system as the reaction equilibrium constant for the formation of $Br_2^{\bullet-}$ ($K = 3.9 \times 10^5\ M^{-1}$) is higher than that of $Cl_2^{\bullet-}$ ($K = 1.4 \times 10^5\ M^{-1}$) in the PC–Cl system [43]. It should be mentioned that the bacterial viability was determined by both direct-count assay and the BacLight™ kit methods to double confirm the inactivation efficiency (Fig. S1). The BacLight™ kit method is a double staining method based on the non-selectivity of SYTO 9 stain towards the integrity of cell membranes and the selectivity of the PI stain towards damaged cell membranes. That is, SYTO 9 can penetrate the cell membrane whatever its integrity to form complex with the living cell DNA to fluoresce green, whereas PI is only able to enter the damaged cells, reducing SYTO 9 fluorescence when both dyes are present, which makes the dead cells emit red light [11]. It should be noted that the orange colored cell images shown in Fig. S1 are actually the effect of mixing green and red colors, visualizing a limited permeability of PI through less damaged cell membranes.

To better understand the inactivation mechanism, FESEM was employed to examine the location and extent damages to *E. coli* cells attached to the TiO_2 substrate after PC, PC–Cl and PC–Br treatments (Fig. 2). An untreated *E. coli* cell exhibits a well-preserved rod-like shape and intact membrane surface (Fig. 2a). The cell lost its characteristic rod-like shape and showing abnormal wavy surface after subjecting to a 300 s PC treatment (Fig. 2b). This suggests that some damages had occurred to the cell membrane, which is supported by the observed gel-like efflux of intracellular contents (the cycled part in Fig. 2b). The released intracellular contents are from the periplasmic space in the Gram-negative cells [44], suggesting the cell membrane were drastically damaged during the PC treatment. A longer PC treatment of 600 s caused further morphological changes and released more intracellular contents because the cell membrane being blasted at this stage of treatment (Fig. 2c). With a 900 s PC treatment, the cytoplasm was completely burst and the outer cell membrane peeled off, leading to a massive amount of intracellular contents being released (Fig. 2d). It is to note that although obvious damages to the cell membrane were observed, the decomposition of the damaged membrane was not obvious. Figs. 2e to h are the FESEM imagines of PC–Cl treated cells. Compared to the PC treated cells, similar damages to the cell membrane (Figs. 2e and f) were observed when the treatment time was short (e.g., 150 and 300 s). However, with longer treatment (e.g., 600 and 900 s), the observed damages are mainly in a form of direct outer membrane decomposition, resulting the exposed cell surface being porous (Figs. 2 g and h), which are very different to the case of PC treated cells. This may suggest that although similar inactivation efficiencies were obtained from PC and PC–Cl treatment samples, the inactivation pathway of PC and PC–Cl treatment processes could be different. These differences are likely due to the presence of different bactericides (oxidative species) in PC and PC–Cl treatment systems. For PC system, AOSs such as $^{\bullet}OH/H_2O_2$ are the major bactericides responsible for cell death while for PC–Cl, other than AOSs, $Cl^{\bullet-}/Cl_2^{\bullet-}$ may play an important role. The relatively long-lived $Cl_2^{\bullet-}$ with stronger oxidation power than that of AOSs could survive the solution process to decompose exposed body parts of the cell [23]. FESEM imagines of PC–Br treated cells are given in Figs. 2i to l. It was found that the observed damages from PC–Br treated cells were more substantial comparing to the PC–Cl treated cells at a corresponding treatment time, which could be used to support the observed high inactivation efficiency of PC–Br method. Nevertheless, the forms of damages observed from PC–Br treated cells were similar to that of PC–Cl treated cells, suggesting a similar

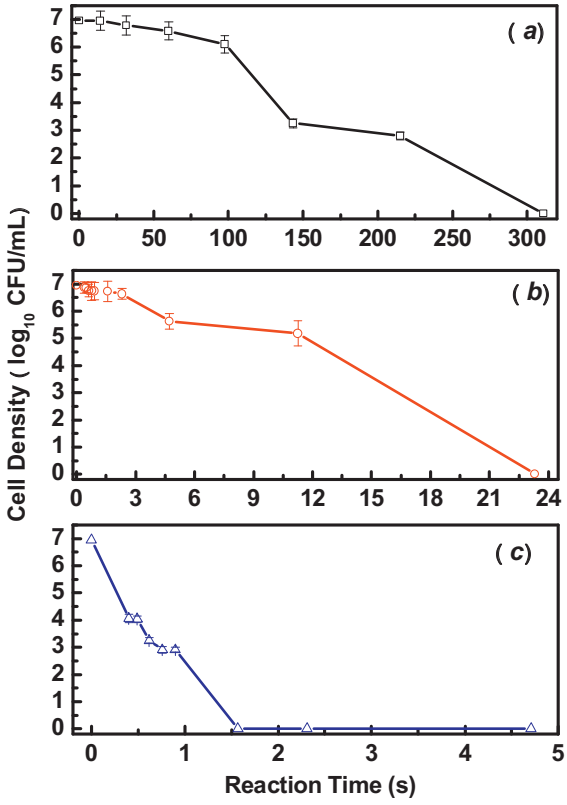

Fig. 3. Survived *E. coli* after different photoelectrocatalytic treatment plot against resident time. (a) PEC treatment; (b) PEC–Cl treatment; and (c) PEC–Br treatment.

inactivation and decomposition pathway for both methods due to the presence of di-halide radical anions ($X_2^{\bullet -}$).

3.2. PEC inactivation with and without halide ions

It has been confirmed that for a PEC system, the applied potential bias serves as an external driving force to timely remove the photoelectrons from TiO_2 conduction band that suppresses the recombination and prolongs the lifetime of photoholes [30]. It is well-known that a photocatalytically generated hole at TiO_2 valence band is a more powerful oxidant than that of AOSs. In a PC system, the photoholes are mainly consumed to generate AOSs rather than directly reacting with the target species [9,11,13]. However, the prolonged photoholes' lifetime in a PEC system can directly react with target species to significantly enhance the photocatalytic efficiency [30]. The bactericidal performance of PEC systems in presence and absence of halide ions were hence investigated to evaluate whether such advantageous features also benefit the inactivation of bacteria. It should be noted that except the applied potential bias, all PEC experiments carried out in this section were under identical conditions as used for PC experiments with the same photoanode, same reactor, same light source and light intensity, same concentration of bacteria and solution composition, and same experimental procedure. The results obtained under such circumstances can be used to meaningfully compare the bactericidal performance of PC and PEC systems.

Fig. 3 shows the plot of inactivation efficiency against reaction time obtained from PEC (with a +0.3 V applied potential bias) treated samples containing 9.0×10^6 CFU/ml *E. coli* in absence and presence of halide ions. It can be seen that for all cases, the obtained PEC bactericidal efficiencies are significantly higher than that of PC methods, attributing to the suppressed the recombination and prolonged photohole lifetime [30]. In case of the PEC inactivation in absence of halide ions, about 3.7 log reduction of *E. coli* can be achieved within 143 s (Fig. 3a), 10 times quicker than that of the PC method. And the time needed to completely inactivate all bacterial cells by PEC is only 311 s. The PEC efficiency enhancement is also well confirmed by the results of membrane integrity assay (Figs. S2a to S2c). Fig. 3b shows the PEC–Cl inactivation efficiency in presence of 1.0 mM Cl^-. It requires only 23.3 s to achieve 100% inactivation, 13 times faster than that of the PEC method in absence of Cl^-. This is in strong contrast to PC treatment process where very similar inactivation efficiencies were obtained in presence and absence of Cl^-. Higher PEC oxidation efficiency toward Cl^- to form $Cl^\bullet$ and $Cl_2^{\bullet -}$ is a likely attribute to the enhanced PEC–Cl inactivation efficiency. Compared to a PC method, a PEC method possessing higher oxidation efficiency toward Cl^- could be due to the ability of direct photohole reaction with Cl^- because of the strong oxidation power and prolonged lifetime of photoholes [30,45]. A dramatically improved bactericidal efficiency was obtained from PEC–Br treated samples (Fig. 3c). In presence of 1.0 mM Br^-, total reduction of *E. coli* can be achieved within 1.57 s. To achieve the same bactericidal effect, the PEC–Br method is more than 190 times faster than that of the PEC treatment in absence of halide ions. Comparing to the PEC–Cl treatment in presence of 1.0 mM Cl^-, to achieve completely inactivation, the PEC–Br treatment is about 15 times faster. Such a superior bactericidal efficiency of PEC-Br method can be largely attributed to the effectiveness of the photoelectrocatalytically generated new bactericides such as $Br^\bullet$ and $Br_2^{\bullet -}$ [23]. Comparing to the time required to achieve 100% inactivation of 9.0×10^6 CFU/mL *E. coli* by PC–Br treatments, the PEC–Br method is more than 760 times faster than that of the PC–Br treatment in presence of 1.0 mM Br^-. In addition, the bacterial viability of PEC–X was also determined by the BacLight™ kit methods to double confirm the inactivation efficiency (Fig. S2).

FESEM images of PEC, PEC–Cl and PEC–Br treated samples were obtained to examine the location and extent damages to *E. coli* cells attached to the TiO_2 substrate (Fig. 4). With a short PEC treatment time (e.g., 30 s) in absence of halide ions, the cell shrinkage depression was clearly visible (Fig. 4a). Unlike the released gel-like cell contents after PC and PC–X treatments (Fig. 2), the released cell contents for PEC treated cells are silk-like appearance (Fig. 4a, cycled), which might be the nuclear acid [46]. This may indicate that both outer and inner cell membranes were damaged by PEC treatment, suggesting a strong oxidation power of the PEC treatment originated from the direct photohole reactions [23,30]. A 60 s PEC treated cell became a 'fried-egg' shape that consists of a thick central core surrounded by a thin gel-like periphery (Fig. 4b). However, no visible damage to the cell body that is not in direct contact to the photoanode surface. This is because the photoholes can only exist within the TiO_2 photocatalyst, and AOSs could not cause visible damage within 60 s of treatment time. Large amount of released silk-like cell contents was observed from cells subjected to a 150 s PEC treatment (Fig. 4c). At this stage, the thin gel-like periphery shown in Fig. 4b was almost disappeared because of rapid decomposition [23,47]. When the PEC treatment time was extended to 300 s, the vicinity spilled out cell contents, the edge of the cell and the cell body part in direct contact to the photoanode were decomposed while the other parts of the cell body were damaged to a much less extent (Fig. 4d). The severe decomposition to the cell body in direct contact with the photoanode indicates the important role of direct photohole reactions and the less damages to other parts of cell body not in direct contact to the photoanode suggests the AOSs has less oxidation power than that of photoholes.

Figs. 4e - h show the SEM images of PEC–Cl treated *E. coli* cells. Initially, small protuberances and shrinkage depressions on the cell surface can be observed (Fig. 4e). The form of the damages with an increased treatment time of 60 s (Fig. 4f) was found to be similar to the 900 s PC–Cl treated samples. At this stage, the exposed

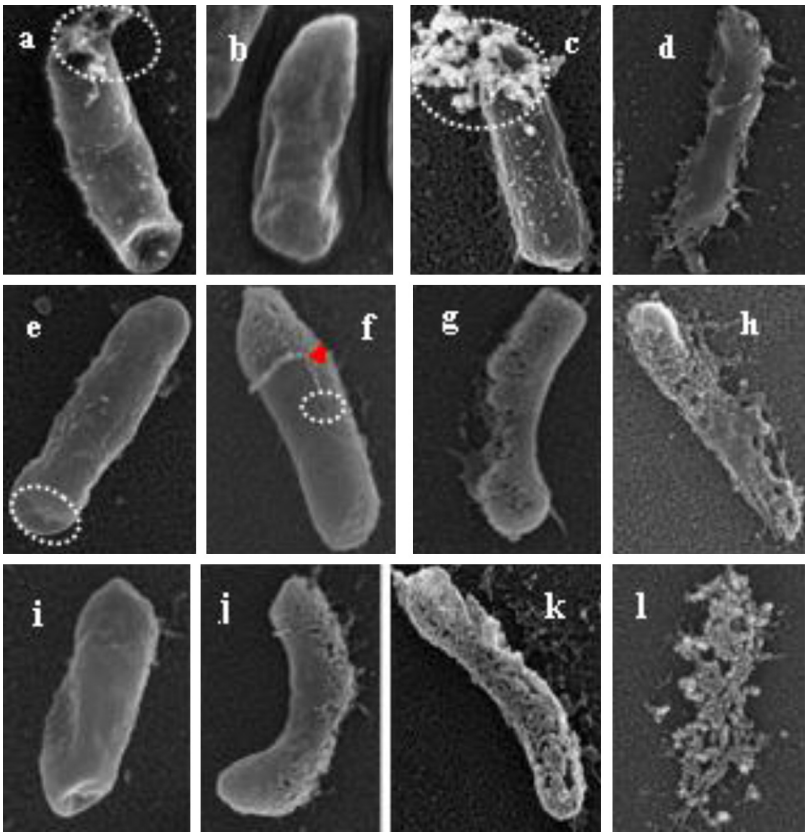

Fig. 4. FESEM images of *E. coli* cell immobilized on the TiO_2 photoanode. (a) After PEC 30 s; (b) PEC 60 s; (c) PEC 150 s; (d) PEC 300 s; (e) PEC–Cl 30 s; (f) PEC–Cl 60 s; (g) PEC–Cl 150 s; (h) PEC–Cl 300 s; (i) PEC–Br 30 s; (j) PEC–Br 60 s; (k) PEC–Br 150 s; and (l) PEC–Br 300 s.

parts of the cell body appeared to be porous, resulting from the membrane and inner structures decomposition by the $Cl^{\bullet -}/Cl_2^{\bullet -}$. A further increased treatment time led to a completely decomposed outer membrane (Fig. 4 g) and large portion of entire cell body (Fig. 4 h). Comparing these observations with those of PC–Cl treated samples, it is obvious that the both processes share a similar decomposition pathway because of the presence common bactericides ($Cl^{\bullet -}/Cl_2^{\bullet -}$). The extend of damages observed from PEC–Cl treated samples were more severe than that of PC–Cl treated samples under comparable treatment time, which could be attributed to the ability of PEC method to suppress recombination, direct photohole reaction and high efficiency of converting Cl^- into $Cl^{\bullet -}/Cl_2^{\bullet -}$.

Representative SEM images of PEC–Br treated *E. coli* cells are also shown in Figs. 4i - l. Comparing to the PEC–Cl treated cells at a corresponding treatment time, the observed damages from PEC–Br treated cells were found to be noticeably severe. Majority cell body can be decomposed after 300 s of PEC treatment (Fig. 4l), suggesting the PEC–Br system is a more effective system than that of PEC–Cl system. However, the forms of damages were almost identical, suggesting the decomposition pathway of the two methods is similar, which is again attributed to the presences of di-halide free radical anions.

3.3. Further discussion

The results and discussion presented so far have confirmed the important role of di-halide anions free radicals played in bactericidal processes. Although the dramatically enhanced bactericidal effect was demonstrated in presence of halide ions, it is unquestionably that as an important class of bactericides, the photocatalytically generated AOSs are also critical to the inactivation performance. An interesting question then arises: how important are AOSs for the inactivation performance of PC–X or PEC–X system? It is well known that the rate of photocatalytic oxidation of water at the UV illuminated TiO_2 can be sharply increased when pH is above 10 [48,49], leading to a higher rate of AOSs production at high pH. This could be used to sort out the relative contribution of AOSs to the inactivation performance of PC–X or PEC–X system. Fig. 5 shows the effect of pH on the percentage inactivation for PC and PEC systems with and without halide ions. The pH range (pH 5.6–9.3) investigated would cover most natural waters. Fig. 5a shows the case without presence of halide ions. The inactivation efficiencies derived from 60.06 s PEC and 97.48 s PC treated samples were used to evaluate the pH effect. The observed inactivation efficiencies were found to increase with pH for both methods. These enhancements in the inactivation efficiency could be largely attributed to the increased rate of AOSs production at higher pH. The extent of the pH effect to PC method was greater than that to PEC method, for example, at pH 5.6, a 97.48 s PC treated sample achieved only 13.9% inactivation but a 99.6% inactivation can be achieved at pH 9.3. This is because the AOSs are the sole class of bactericides in a PC process so any increase in AOSs production will be directly reflected in the inactivation performance. Fig. 5b shows the case with presence of Cl^-. The inactivation efficiencies derived from 1.16 s PEC–Cl and 97.48 s PC–Cl treated samples were used for the evaluation. It was found that for the PEC–Cl treated samples under different pHs, the inactivation percentage moderately increased from 38.8% to 52.5% when pH increased from 5.6 to 7.4, but dramatically increased to 99.0% when pH was further increased to 9.3, suggesting a significant contribution by AOSs at high pH. For PC–Cl treated samples, an almost linearly increased inactivation percentage was observed for the pH range investigated, suggesting a significant contribution of AOSs toward inactivation. Fig. 5c shows the cases with presence of Br^-. The inactivation efficiencies

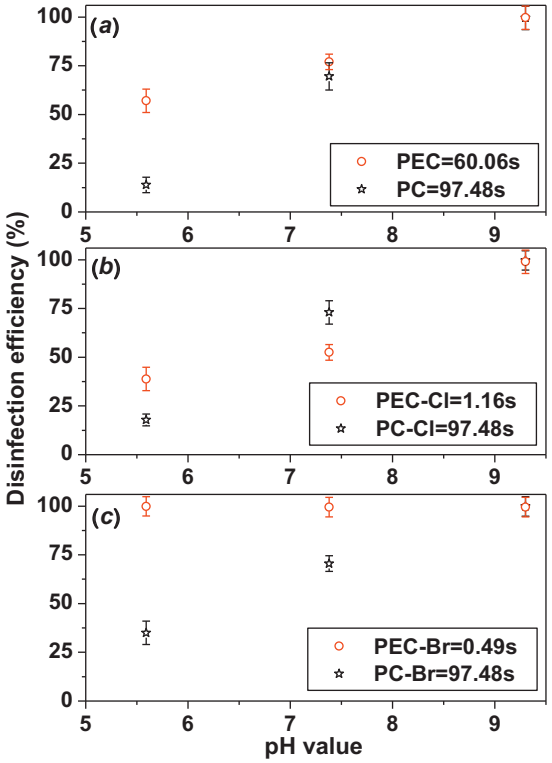

Fig. 5. Effect of pH on the (a) PC and PEC; (b) PC–Cl and PEC–Cl; and (c) PC–Br and PEC–Br bactericidal efficiencies of *E. coli* on TiO_2 films.

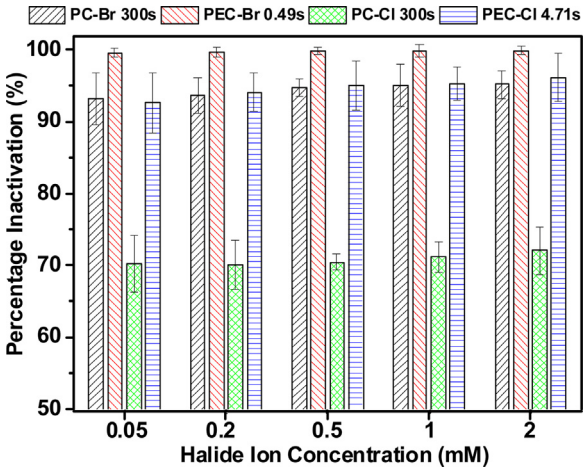

Fig. 6. Effect of halide ion concentration on the PC–Cl, PEC–Cl; PC–Br and PEC–Br bactericidal efficiencies of *E. coli* on TiO_2 films.

derived from 0.49 s PEC–Br and 97.48 s PC–Br treated samples were used for the evaluation. In strong contrast to all other cases investigated, the observed inactivation efficiencies were independent of pH for PEC–Br treated samples, suggesting a dominant role of $Br^{\bullet -}/Br_2^{\bullet -}$ in a PEC–Br inactivation process. For PC–Br treated samples, an almost linearly increased inactivation percentage was observed for the pH range investigated, which is similar to the case of PC–Cl process, suggesting a significant contribution of AOSs.

We have previously proposed that in a bactericidal process, Br^- acts as an "electron mediator" that does not change its chemical form before and after bactericidal process (Eqs. (2) and (3)) [23]. This should also be the case for other halide (X^-) systems. That is:

$$TiO_2 + X^- \xrightarrow{UV} X^{\bullet} \quad (4)$$

$$X^{\bullet} + X^- \rightarrow X_2^{\bullet -} \quad (5)$$

$$X^{\bullet}/X_2^{\bullet -} \xrightarrow{Bacteria} X^- + \text{Oxidized bacteria.} \quad (6)$$

If the halide ion does act as an electron mediator with a sufficient light intensity for which the X^- turnover is not the rate limiting factor, then the observed inactivation efficiency should be relatively independent of X^- concentration. Fig. 6 shows the effect of X^- (X = Cl, Br) concentration on the inactivation efficiency. The inactivation efficiencies derived from 300 s PC–Cl, 4.71 s PEC–Cl, 300 s PC–Br and 0.49 s PEC–Br treated samples were used for the evaluation. For all cases investigated, the changes in X^- concentration from 0.05 to 2 mM have no noticeable effect on the inactivation efficiency. This conclusion is different from the observations of Rincon and Pulgarin [50], where the PC inactivation efficiency was strongly affected by changing Cl^- concentrations. This could be due to the differences in reaction conditions employed. For instance, 0.05–2 mM of Cl^- concentrations was used by us, and 0.02–260 mM was employed by them. Furthermore, in our case, the low concentrations of Cl^- serve as the electron mediator while in their case the high Cl^- concentration might block the active sites of the catalyst surface thus deactivating the catalyst towards biohazards. On the other hand, the bulk reactor was used by them, while a small exhaustive degradation thin-layer reactor was applied in our paper. In addition, no change in X^- concentration was observed before and after inactivation experiments in our previous work [23]. These observations confirm that the halide ion served as an electron mediator during a photocatalytic or photoelectrocatalytic inactivation process, as demonstrated by Eqs. (3)–(6). The data shown in Fig. 6 also suggest that over 99% inactivation efficiency can be readily achieved within 0.49 s by PEC–Br treatment in presence of Br^- concentration as low as 50 μM.

4. Conclusions

In this work, we have demonstrated that new forms of effective bactericides such as $X^{\bullet -}/X_2^{\bullet -}$ can be generated in situ via a photocatalysis or photoelectrocatalysis process. The bactericidal performances of photocatalytic and photoelectrocatalytic systems in absence and presence of low concentrations of X^- have been quantitatively studied and meaningfully compared under identical experimental conditions. The PEC–Br system is the most effective bactericidal system amongst all systems investigated, capable of inactivating 100% of 9.0×10^6 CFU/mL *E. coli* within 1.57 s. The photocatalytically generated AOSs are found to be the important attributes to the bactericidal performance of all cases investigated except the PEC–Br system, where the bactericidal performance is dominated by the photoelectrocatalytically generated $Br^{\bullet -}/Br_2^{\bullet -}$. It has been revealed that in the bactericidal process, X^- acts as an electron mediator that does not change its chemical form before and after bactericidal process, and a high bactericidal performance photoelectrocatalytic system can be established with Br^- concentration as low as 50 μM, which is important for a membrane-based PRW production process as no long-lived oxidative residuals remains in the disinfected solution.

Acknowledgments

Authors thank Dr. Deborah Stenzel for her help on SEM sample preparations, and financial support from Australian Research Council and NSFC (No. 21077104). This is contribution No. IS-1649 from GIGCAS.

Appendix A. Supplementary data

Supplementary data associated with this article can be found, in the online version, at http://dx.doi.org/10.1016/j.apcatb.2013.04.004.

References

[1] Z. Chen, H.H. Ngo, W. Guo, Science of the Total Environment 426 (2012) 13–31.
[2] L.C. Rietveld, D. Norton-Brandao, R. Shang, J. van Agtmaal, J.B. van Lier, Water Science and Technology 64 (2011) 1540–1546.
[3] C. Rodriguez, P. Van Buynder, R. Lugg, P. Blair, B. Devine, A. Cook, P. Weinstein, International Journal of Environmental Research and Public Health 6 (2009) 1174–1209.
[4] J.E. Drewes, M. Reinhard, P. Fox, Water Research 37 (2003) 3612–3621.
[5] M. Jacob, C.C. Li, C. Guigui, C. Cabassud, G. Lavison, L. Moulin, Desalination and Water Treatment 46 (2012) 75–86.
[6] L. Malaeb, G.M. Ayoub, Desalination 267 (2011) 1–8.
[7] T. Matsunaga, R. Tomoda, T. Nakajima, H. Wake, FEMS Microbiology Letters 29 (1985) 211–214.
[8] M.R. Elahifard, S. Rahimnejad, S. Haghighi, M.R. Gholami, Journal of the American Chemical Society 129 (2007) 9552–9553.
[9] O.K. Dalrymple, E. Stefanakos, M.A. Trotz, D.Y. Goswami, Applied Catalysis B: Environmental 98 (2010) 27–38.
[10] D.Q. Zhang, G.S. Li, J.C. Yu, Journal of Materials Chemistry 20 (2010) 4529–4536.
[11] S. Josset, N. Keller, M.C. Lett, M.J. Ledoux, V. Keller, Chemical Society Reviews 37 (2008) 744–755.
[12] L. Liu, Z. Liu, H. Bai, D.D. Sun, Water Research 46 (2012) 1101–1112.
[13] A. Markowska-Szczupak, K. Ulfig, A.W. Morawski, Catalysis Today 169 (2011) 249–257.
[14] H.A. Foster, I.B. Ditta, S. Varghese, A. Steele, Applied Microbiology and Biotechnology 90 (2011) 1847–1868.
[15] M. Gao, T. An, G. Li, X. Nie, H.-Y. Yip, H. Zhao, P.-K. Wong, Water Research 46 (2012) 3951–3957.
[16] D. Wu, H. You, R. Zhang, C. Chen, D. Lee, Bioresource Technology 102 (2011) 9838–9842.
[17] T. Saito, T. Iwase, J. Horie, T. Morioka, Journal of Photochemistry and Photobiology. B 14 (1992) 369–379.
[18] Z.X. Lu, Z.L. Zhang, M.X. Zhang, H.Y. Xie, Z.Q. Tian, P. Chen, H. Huang, D.W. Pang, Journal of Physical Chemistry B 109 (2005) 22663–22666.
[19] K. Sunada, T. Watanabe, K. Hashimoto, Environmental Science and Technology 37 (2003) 4785–4789.
[20] V.A. Nadtochenko, A.G. Rincon, S.E. Stanca, J. Kiwi, Journal of Photochemistry and Photobiology. A 169 (2005) 131–137.
[21] O.K. Dalrymple, W. Isaacs, E. Stefanakos, M.A. Trotz, D.Y. Goswami, Journal of Photochemistry and Photobiology. A 221 (2011) 64–70.
[22] S. Pigeot-Remy, F. Simonet, D. Atlan, J.C. Lazzaroni, C. Guillard, Water Research 46 (2012) 3208–3218.
[23] G.Y. Li, X.L. Liu, H.M. Zhang, T.C. An, S.Q. Zhang, A.R. Carroll, H.J. Zhao, Journal of Catalysis 277 (2011) 88–94.
[24] C. Vacaroiu, M. Enache, M. Gartner, G. Popescu, M. Anastasescu, A. Brezeanu, N. Todorova, T. Giannakopoulou, C. Trapalis, L. Dumitru, World Journal of Microbiology and Biotechnology 25 (2009) 27–31.
[25] K. Shiraishi, H. Koseki, T. Tsurumoto, K. Baba, M. Naito, K. Nakayama, H. Shindo, Surface and Interface Analysis 41 (2009) 17–22.
[26] W.W. Zhang, Y.Q. Chen, S.Q. Yu, S.G. Chen, Y.S. Yin, Thin Solid Films 516 (2008) 4690–4694.
[27] H.T. Yu, X. Quan, Y.N. Zhang, N. Ma, S. Chen, H.M. Zhao, Langmuir 24 (2008) 7599–7604.
[28] M. Cho, E.L. Cates, J. Kim, Water Research 45 (2011) 2104–2110.
[29] N. Baram, D. Starosvetsky, J. Starosvetsky, M. Epshtein, R. Armon, Y. Ein-Eli, Electrochimica Acta 54 (2009) 3381–3386.
[30] H.J. Zhao, D.L. Jiang, S.Q. Zhang, W. Wen, Journal of Catalysis 250 (2007) 102–109.
[31] P.S.M. Dunlop, T.A. McMurray, J.W.J. Hamilton, J.A. Byrne, Journal of Photochemistry and Photobiology. A 196 (2008) 113–119.
[32] P.A. Christensen, T.P. Curtis, T.A. Egerton, S.A.M. Kosa, J.R. Tinlin, Applied Catalysis B 41 (2003) 371–386.
[33] Y.Z. Zhang, X.Y. Xiong, Y. Han, X.H. Zhang, F. Shen, S.H. Deng, H. Xiao, X.Y. Yang, G. Yang, H. Peng, Chemosphere 88 (2012) 145–154.
[34] I.M. Butterfield, P.A. Christensen, T.P. Curtis, J. Gunlazuardi, Water Research 31 (1997) 675–677.
[35] K. Lv, Y.M. Xu, Journal of Physical Chemistry B 110 (2006) 6204–6212.
[36] J.E. Rogers, B. Abraham, A. Rostkowski, L.A. Kelly, Photochemistry and Photobiology 74 (2001) 521–531.
[37] H.J. Zhao, D.L. Jiang, S.Q. Zhang, K. Catterall, R. John, Analytical Chemistry 76 (2004) 155–160.
[38] H. Selcuk, H.Z. Sarikaya, M. Bekbolet, M.A. Anderson, Chemosphere 62 (2006) 715–721.
[39] M.M. Cheng, A. Bakac, Journal of the American Chemical Society 130 (2008) 5600–5605.
[40] G. Merenyi, J. Lind, Journal of the American Chemical Society 116 (1994) 7872–7876.
[41] M.A. Kohanski, D.J. Dwyer, B. Hayete, C.A. Lawrence, J.J. Collins, Cell 130 (2007) 797–810.
[42] A.A. Belaaouaj, K.S. Kim, S.D. Shapiro, Science 289 (2000) 1185–1187.
[43] Y. Liu, A.S. Pimentel, Y. Antoku, B.J. Giles, J.R. Barker, Journal of Physical Chemistry A 106 (2002) 11075–11082.
[44] D.M. Blake, P.C. Maness, Z. Huang, E.J. Wolfrum, J. Huang, W.A. Jacoby, Separation and Purification Methods 28 (1999) 1–50.
[45] S.Q. Zhang, H.J. Zhao, Analyst 133 (2008) 1684–1691.
[46] N.A. Campbell, J.B. Reece, N. Meyers (Eds.), Biology, seventh ed., Benjamin Cummings, San Francisco, 2004.
[47] L.X. Pinho, J. Azevedo, V.M. Vasconcelos, V.J.P. Vilar, R.A.R. Boaventura, Journal of Advanced Oxidation Technologies 15 (2012) 98–106.
[48] S.Q. Zhang, L.H. Li, H.J. Zhao, Environmental Science and Technology 43 (2009) 7810–7815.
[49] S.Q. Zhang, H.J. Zhao, D.L. Jiang, R. John, Analytica Chimica Acta 514 (2004) 89–97.
[50] A.G. Rincon, C. Pulgarin, Applied Catalysis B 51 (2004) 283–302.